IOSUD - Universitatea Politehnica Timişoara
Şcoala Doctorală de Studii Inginereşti

CONTRIBUȚII LA EVALUAREA ȘI AMELIORAREA EMISIILOR ȘI IMUNITĂȚII ÎN COMPATIBILITATEA ELECTROMAGNETICĂ A AUTOVEHICULELOR RUTIERE

CONTRIBUTIONS TO THE EVALUATION AND IMPROVEMENT OF EMISSIONS AND IMMUNITY IN ELECTROMAGNETIC COMPATIBILITY OF ROAD VEHICLES

Teză de doctorat – Rezumat în limba engleză
pentru obținerea titlului științific de doctor la
Universitatea Politehnica Timișoara
în domeniul de doctorat inginerie electronică, telecomunicații și tehnologii informaționale

autor ing. Andrei-Marius SILAGHI
conducător științific Prof.univ.dr.ing. Aldo De SABATA

luna iunie anul 2019

The PhD thesis is structured in 5 chapters: in Chapter 1 the standards in the field of Electromagnetic Compatibility are described; Chapter 2 presents contributions to automotive emissions; Chapter 3 presents solutions for improving immunity in the automotive field; applications of metamaterials are described in Chapter 4 and the conclusions and contributions are presented in the final chapter.

1. Standards from the field of Electromagnetic Compatibility of Road Vehicles

In the introductory chapter the relevant aspects of the two standards that are used mainly in the field of Electromagnetic Compatibility of road vehicles: CISPR 25 and ISO 11452 are presented and commented on. The following test methods are covered by the CISPR 25 standard: cadiated emission tests (with Absorber Lined Shielded Enclosure and Stripline), conducted emission tests with current probe and conducted emissios – voltage method [1], [2]. Also from ISO 11452 the following sub-parts are described: ISO 11452 (Absorbent Lined Shielded Enclosure), ISO 11452-4 (Bulk Current Injection) and ISO 11452-5 (Stripline) [3] - [6].

2. Contributions to the Improvement of Emissions in Electromagnetic Compatibility of Road Vehicles

The validation of the electromagnetic compatibility of road vehicles requires the passing of electromagnetic immunity and emissions tests. Electromagnetic emissions can be radiated or conducted. The CISPR 25 standard specifies the frequency range and the equipment used for the testing of radiated and conducted emissions in Automotive.

In Chapter 2, we present the main Electromagnetic Compatibility Tests regarding radiated and conducted emissions in the Automotive Industry. Instead of a general theoretical presentation, easy to find in the literature, I chose to describe and comment on the concrete tests I took part and to evaluate and ameliorate them from different points of view, taking into account uncertainty and repeatability. We also present our own contributions to this issue so far.

Measuring Radiated Emissions (RE) by Devices Under Test (DUT) is one of the stages of Electromagnetic Compatibility tests. In this chapter, a measurement setup for the radiated emissions produced by an electronic module in the car is described, studied and improved. In fig. 1 it is noted that the peak detector provided a value above the quasi-peak limit, so we performed a new quasi-peak detector measurement (fig. 2). The value of the quasi-peak detector was below the quasi-peak limit. So, in terms of radiated emissions, the DUT is declared to be appropriate (pass) [7].

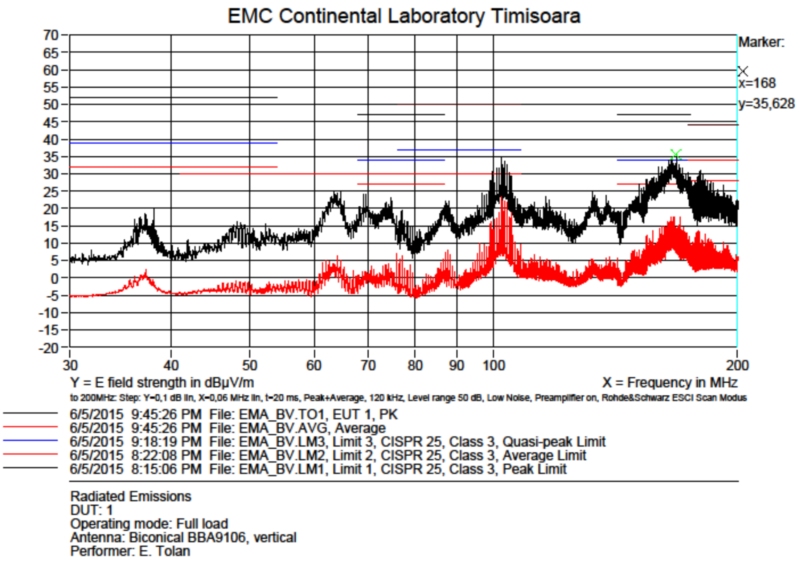

Fig. 1 Measurement of DUT with biconical antenna. Peak and average values [7]

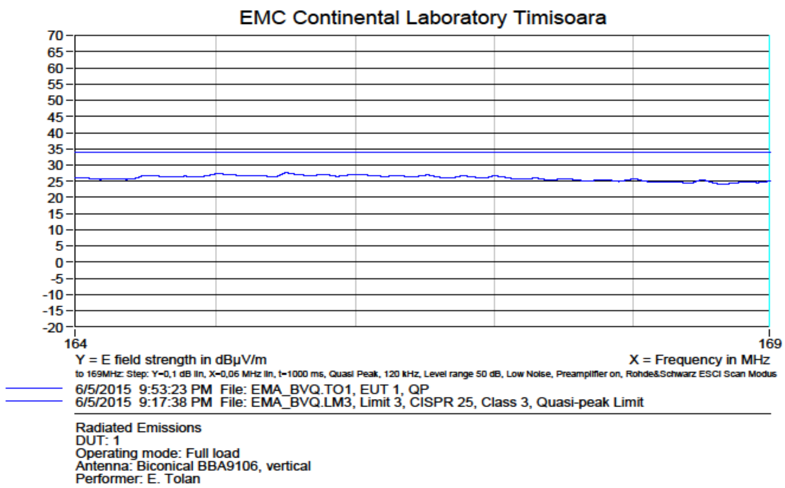

Fig. 2 Re-measurement with quasi-peak detector was made for the frequencies at which the peak detector exceeded the limit for quasi-peak [7]

In this work it is also investigated the differences that occur when different measuring antennas and different semi-anechoic chambers, named ALSE 1 and ALSE 2, are used in the radiated emission tests performed on the same DUT. For radiated emissions testing, we used the following antennas: two monopole antennas (Monopole VAMP9243 and RodAntenna HFZ2-Z6) in the range of 0.1-30 MHz, two biconical antennas (Schwarzbeck biconical BBA9106 and Biconical HK116E) between 30-200 MHz, two log-periodic antennas (Logger VUSLP9111B and Logper HL223) from 200 MHz to 1 GHz and two log-periodic antennas (Logper VUSLP9111B and LogPer HL050) from 1 GHz to 3.2 GHz.

In fig. 3 we can observe the measurement configuration with the monopole antenna. The measurements reported in fig. 4 covered the frequency range 100 KHz to 30 MHz and were based on a vertically polarized monopole antenna. The results obtained in ALSE 2 are represented by black (peak detector) and red (average value detector). Results from ALSE1 are represented by brown (peak detector) and green (average value detector).

All the figures mentioned in this sub-chapter, and the suplimentary ones from the thesis show that the results of the measurements are not identical, irrespective of the bandwidth and the antennas used. In fig. 4, there are obvious significant differences that may arise from the different drivers used by the two measuring receivers. In the case of R&S ESCI we used the FFT method from 3.5 MHz and receiver mode from 100KHz to 3.5MHz. R&S ESR 7 uses FFT method across the entire frequency range. We can conclude that the results of the measurements depend on the configuration of the tests, sometimes significantly, although the equipment meets the requirements of the standards [8].

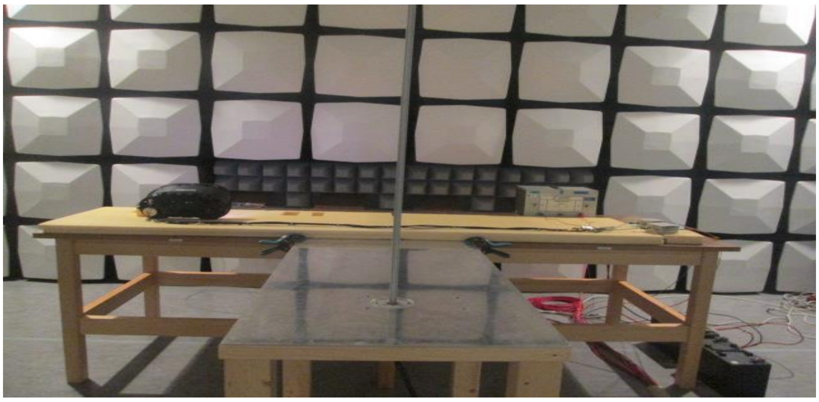

Fig. 3 Monopole antenna test configuration [8]

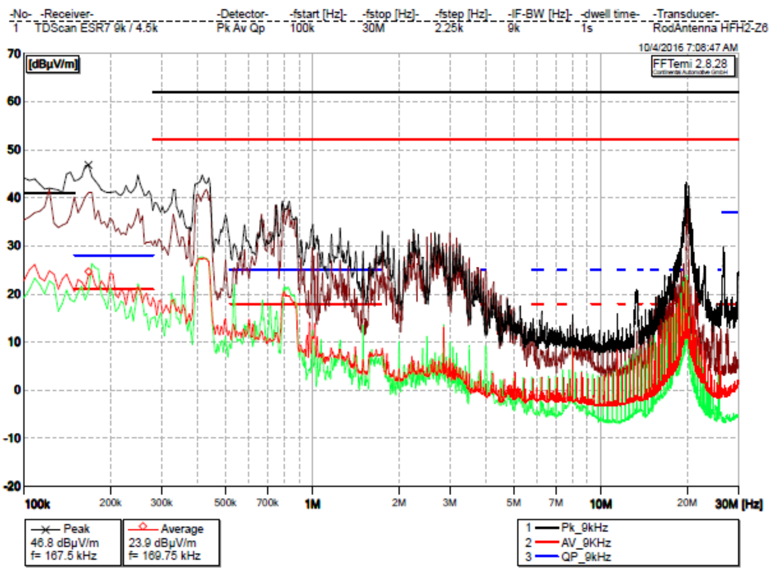

Fig. 4 Measurement with monopole antenna. Peak and average values [8]

The measurement of Conducted Emissions (CE) is another important test in the validation of Electromagnetic Compatibility of road vehicles. In this sub-chapter, several case studies are also presented and commented and various methods can be used to reduce the CE levels: connecting capacitors between 10 and 220 nF on the middle, left and right screws of the PCB (the screws to which the metallic PCB chassis is attached); removing mechanical capacitors and also replacing coils with some shielded ones. In fig. 5 we can notice an initial failed test. We can see the spikes measured with the average value detector in correspondence with the spikes from the peak detector measurement, and the peak level is over the narrow band limit in that place. Fig. 6 shows the result of another solution that solves the problem at 1 MHz. It consists in removing mechanical capacitors [9].

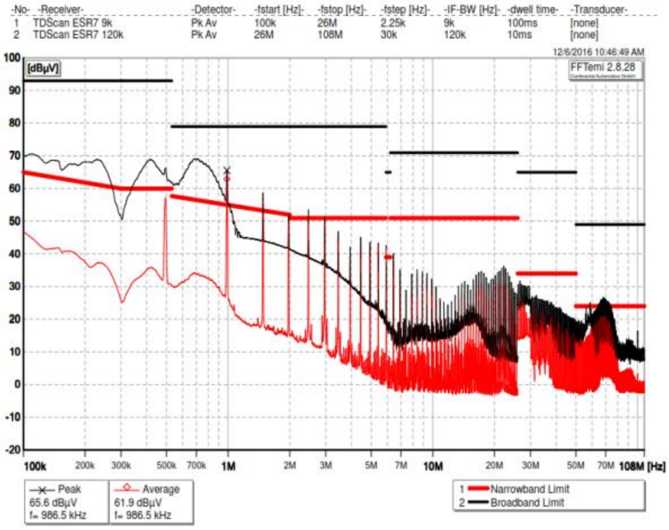

Fig. 5 Initial measurement [9]

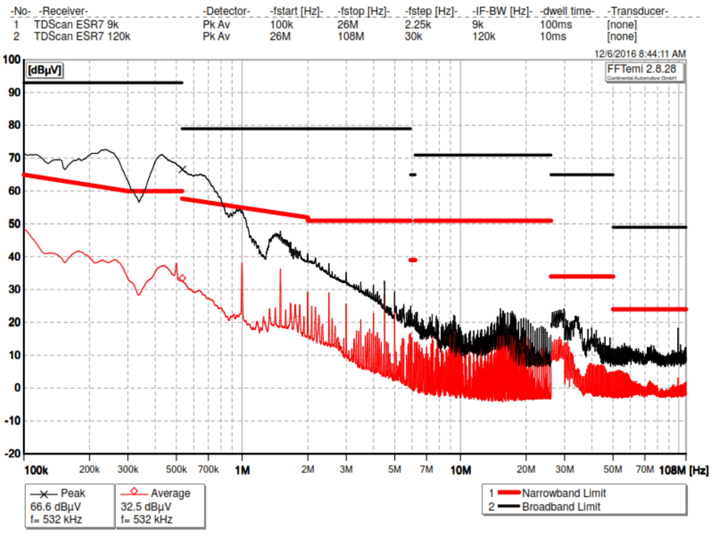

Fig. 6 Measurement results after the removal of mechanical capacitors [9]

Also in Chapter 2, a near-field scanning technique is presented in order to reduce RE levels, so as to reduce the product's time to market. In fig. 7 an initial test that is a fail is reported. We can see that the value measured by the peak detector is above the narrow band limit at 831.25 kHz, so we also measured the average value detector. The difference between the peak detector (28.8 dBuV / m) and the average detector (26.3 dBuV / m) at this frequency is below

6 dB, so we can conclude that the test is a fail. To find a solution so that the product can pass RE tests, I used the near field scanning system EHX + to find the emission source.

We started with a spatial scan of the entire DUT to find the location with the highest emissions (fig. 8). Within a spatial scan, a frequency of interest must be selected (in our case 831 kHz), for which the magnetic field is calculated. By comparing this spatial scan with the layout of the project, we have discovered where the emissions originated. The DUT consisted of a two-layer PCB, hereinafter referred to as the bottom and top layer.

Then we did a spectral scan (fig. 9) at the same location and found that the fundamental frequency of the picked signal coming from that place is 415.5 KHz. In the far field test, we can see this fundamental frequency, but the second harmonic has a much greater influence because of the lower limit imposed by OEM in the 0.5-2 MHz frequency range.

After the near field investigations, a final test was conducted in the semi-anecoic chamber. This test (fig. 10) is a test passed with success since, at the same frequency (831 kHz), the peak detector provides a value over the narrow band limit, but the difference between peak detectors (29 dBuV / m) and average detector (21.7 dBuV / m) is greater than 6 dB [10].

So, using a near-field scanning technique, we found the emission source and we were able to find a solution so that the electronic device could pass the OEM limits at RE test. Also, using this solution, a cheaper and simpler method was adopted compared to several tests in a semi-anechoic room that would have been otherwise needed.

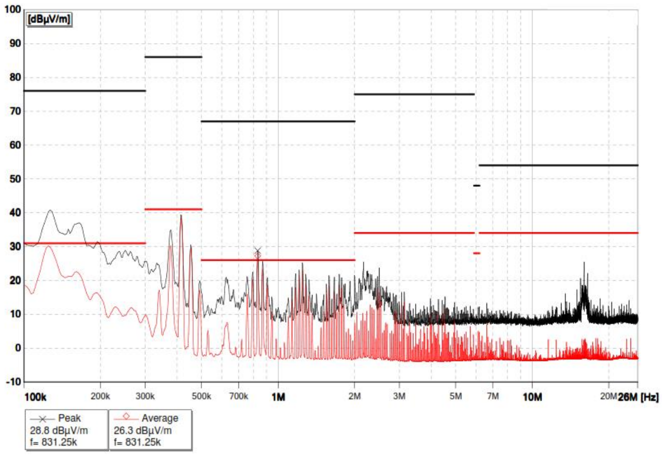

Fig. 7 Initial fail measurement results of radiated emissions test. Peak and average values [10]

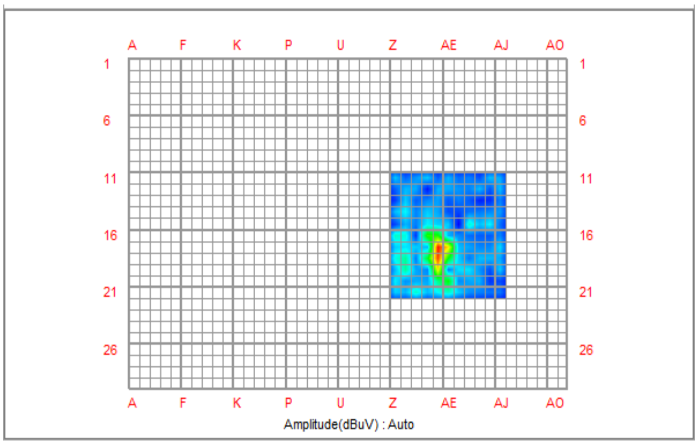

Fig. 8 Spatial scan with EHX+ [10]

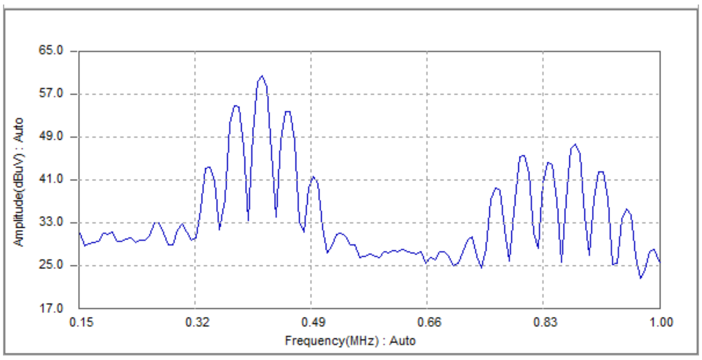

Fig. 9 Spectral scan with EHX+ [10]

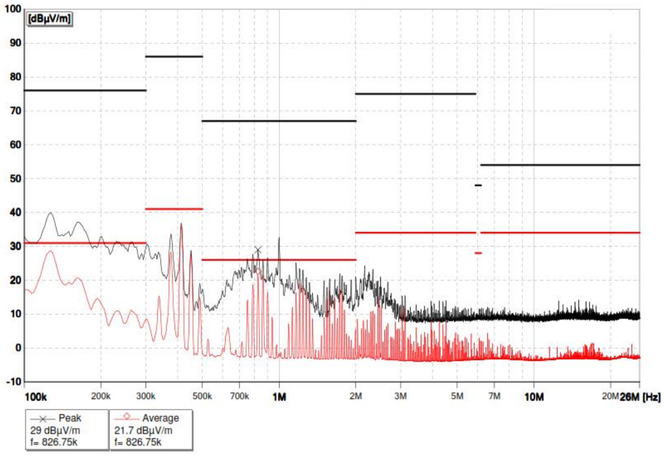

Fig. 10 Final test which is a pass. Peak and average values [10]

The relevance of EMC tests must be ensured by their repeatability both within the same laboratory and between different laboratories. One of the most important elements in the tests is the semi-anecoic chamber (ALSE). It is necessary that the parameters of the chambers belonging to different laboratories are within the same limits, otherwise the tests performed on the same product will have different results in different laboratories.

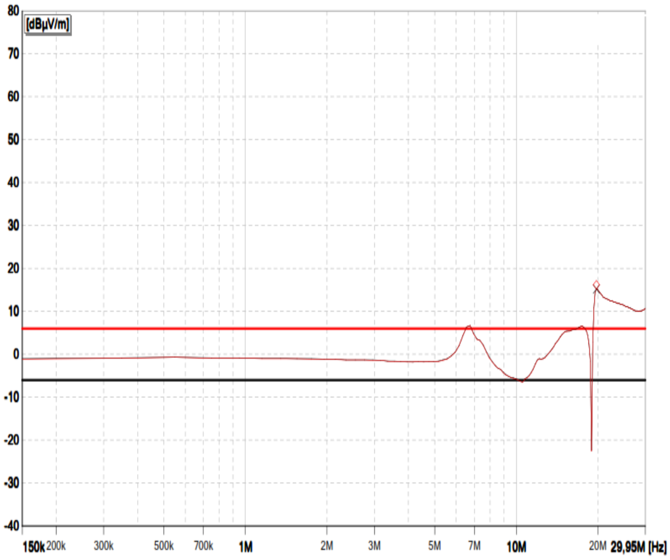

Fig. 11 The test cycle with monopole antenna and without ferrites [11]

Ensuring that this requirement is met is called chamber validation. In the following part, in this chapter, a method for validating the semi-anechoic chamber where the emission tests are carried out is presented and discussed and the results are compared with those obtained in other laboratories [11].

During the measurements a total of 481 frequencies were used as follows: 150 frequencies in the range (150 kHz - 29.95 MHz), 170 frequencies in the range (30 MHz to 199 MHz) and 161 frequencies in the range (200 MHz - 1000 MHz). In Appendix J of CISPR 25 standard it is specified that at least 90% of the measured data must be between -6dB and + 6dB limits in regard to the average, so from a total of 481 points, a minimum of 433 points must adhere to this tolerance (only a maximum of 55 points may exceed the limit). The first test cycle was performed without corrections for the -6dB and + 6dB limits. The second cycle was performed without ferrite (fig.11) and resulted in 70 peaks being outside the tolerance limit. The third cycle (done with ferrite) was saved in the validation (fig. 12) and showed that only 21 peaks were outside the limits, and 129 were inside [11].

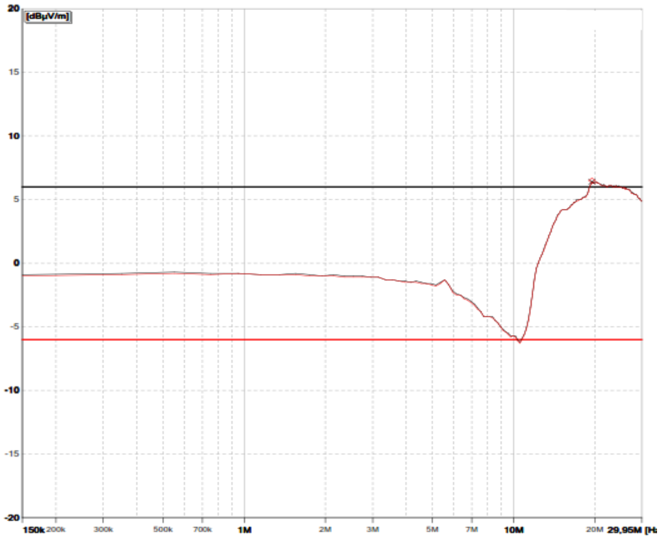

Fig. 12 The test cycle with monopole antenna [11]

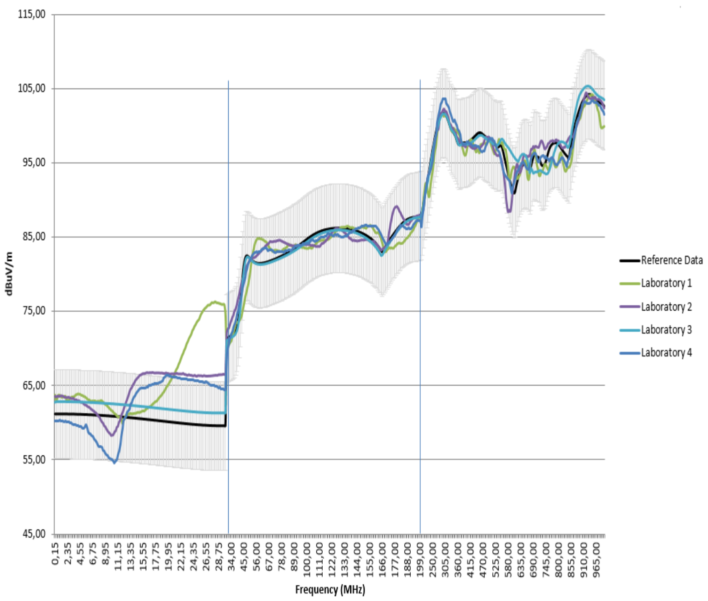

Fig. 13 Reference values vs. measured values [11]

The second measurement was done with the biconical and log-periodic antennas: 30 MHz - 1 GHz. All peaks (331) respected the internal tolerance limit at the first pass. Thus, out of a total of 481 points, 460 were within the tolerance range of -6dB and + 6dB, resulting in a total of 95% of the measured data, which is in accordance with CISPR 25, Appendix J.

After the reported measurements, the radiator was sent to three other ALSE locations. This first ALSE will be named below: Laboratory 4, and the other will be Laboratory 1, 2 and 3. Fig. 13 is the graph containing the data measured by each laboratory, corresponding to the entire frequency range, as compared to the reference data, including the +/- 6dB limits. From the above figure some conclusions can be drawn. As for monopole antenna measurements, Laboratory 1 shows large variations for frequencies between 20 and 29 MHz compared to the reference values. In terms of biconical antenna measurements and log-period antenna, all laboratories appear to fall within the tolerance of the reference data.

3. Contributions to the Improvement of Immunity in Electromagnetic Compatibility of Automotive Industry

In subchapter 3.2 we presented key concepts for immunity testing. We started with the definition of immunity and continued with the chain of equipment used for testing in accordance with ISO 11452-2. We conducted a radiated immunity test on a Automotive DUT to assess its performance in the presence of an electromagnetic field inside a semi-anecoic chamber.

We presented the results of the measurements obtained with two different types of antennas in our laboratory: the log-periodic antenna and the horn antenna. An example of a test can be seen in fig. 14. On the basis of these results, we have paved the way for more realistic calibration methods and test procedures with improved reliability because the equipment parameters are known by measurement and not only by the data provided by the manufacturer [12].

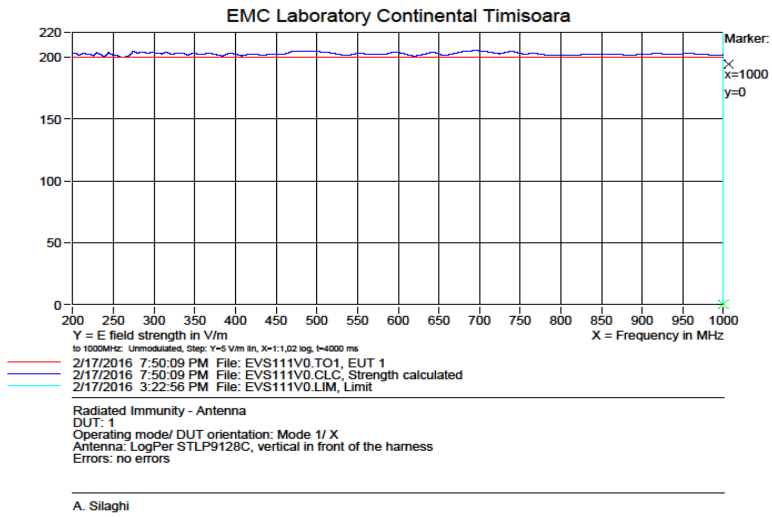

Fig. 14 Generation of CW (unmodulated sinusoidal wave) [12]

In sub-chapter 3.3 we presented some key concepts for testing immunity to portable transmitters. I started with the presentation of the procedure used for testing: ISO-11452-9. After that, we compared two directional couplers to see which one is best suited to this application.

I also measured the VSWR (fig. 15, example for the 52 MHz antenna) and I presented the Smith diagrams (fig. 16, example for 125 MHz) for the three helical antennas commonly used for immunity testing to see if these correspond to the nominal values provided by the manufacturer.

Finally, we made tests with the two directional couplers and the three antennas and concluded that we need to use a Werlatone coupler to achieve more realistic results (fig. 17). We demonstrated the need to rely on the measured parameters of the equipment instead of the nominal values to avoid the potential false results of the immunity tests. In future work, we will use the results reported in the development and introduction of corrective procedures to allow for the correct conduct of the tests [13].

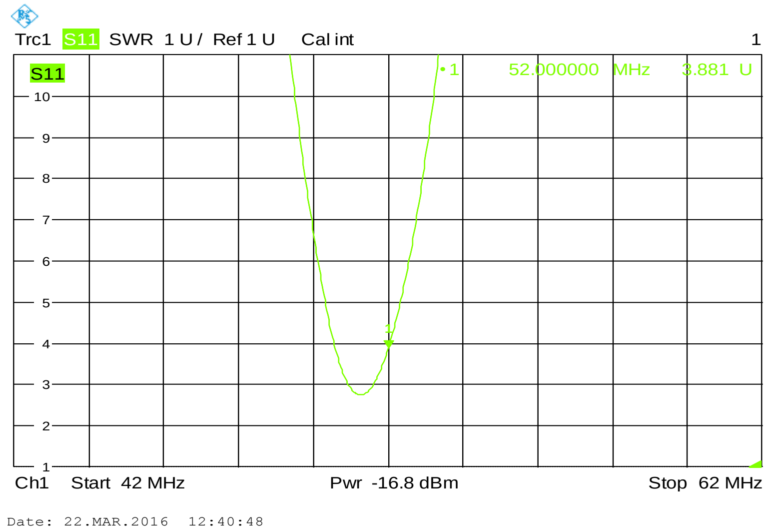

Fig. 15 VSWR for NMHA 52MHz antenna [13]

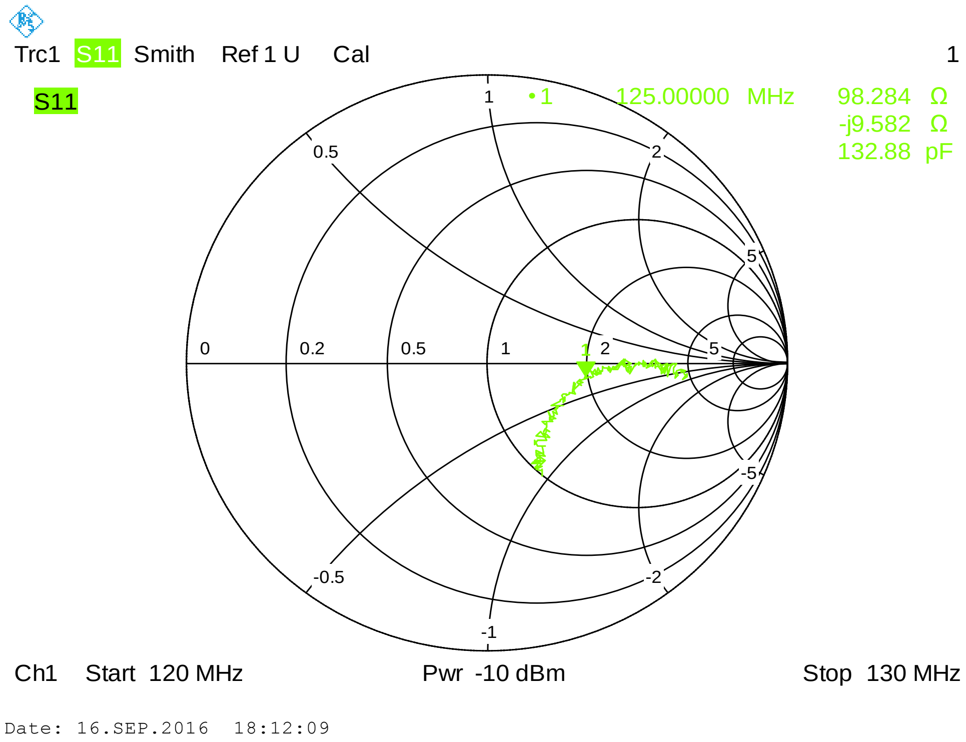

Fig. 16 Smith chart for NMHA 125MHz antenna [13]

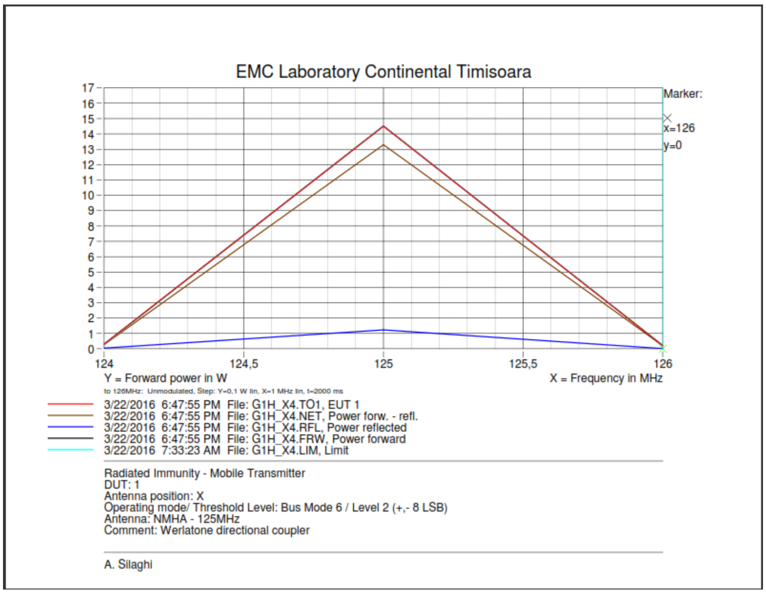

Fig. 17 Test with the help of Werlatone coupler (NMHA 125MHz antenna) [13]

In subchapter 3.4 we tested the effects of CW, FM and analogue TV signals on DVB-T and DVB-C channels that acted as additive noise. The first conclusion is that for the same power injected into the channel, Gaussian noise leads to the greatest deterioration of the BER. During the experiments, we observed that, due to OFDM multiplexing, the DVB-T channel behaves differently from the DVB-C channel: in DVB-T, a spectrum scatter by modulation decreases BER, while DVB-C is more sensitive to modulation, but has a higher immunity to CW signals. In the case of the DVB-T signal, the ATV interferer can be assimilated to a CW interferer, but in the case of DVB-C an ATV interferer is closer to Gaussian noise [14], [15].

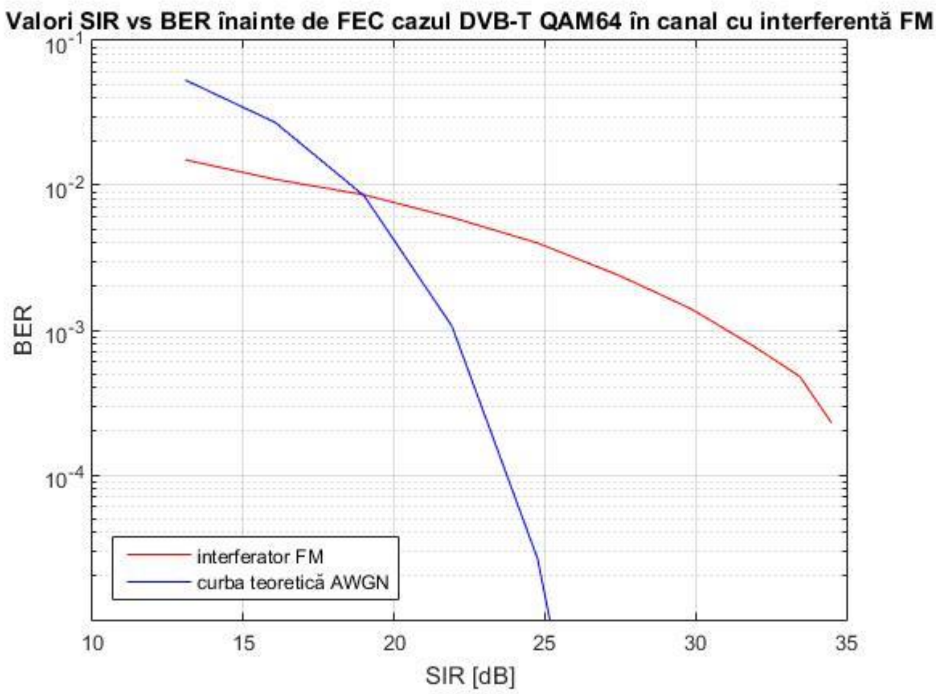

Fig. 18 BER of the signal DVB-T QAM64 interfered with FM signal, compared with the theoretical function AWGN BER [14]

In all cases, the AWGN interferer represents an upper limit, leading to the worst deterioration to the BER compared to the tested signals, for the same injected power interference.

In fig. 18 (DVB-T case) we compared the BER vs. SIR function corresponding to the same signal with the theoretical equivalents BER vs. E_b/N_o for AWGN (Additive White Gaussian Noise), replacing SIR with BER. E_b represents the energy per bit and N_0 represents the spectral density of the noise power.

As can be seen in fig. 19 (DVB-C case), the BER for the theoretical AWGN case is much higher than for the case of interference with the power level equivalent to the AWGN case of the ATV signal. In conclusion, regarding constellations, the interferer is clearly visible if the ATV is unmodulated and scatters around the constellation if the modulation is used (fig. 20).

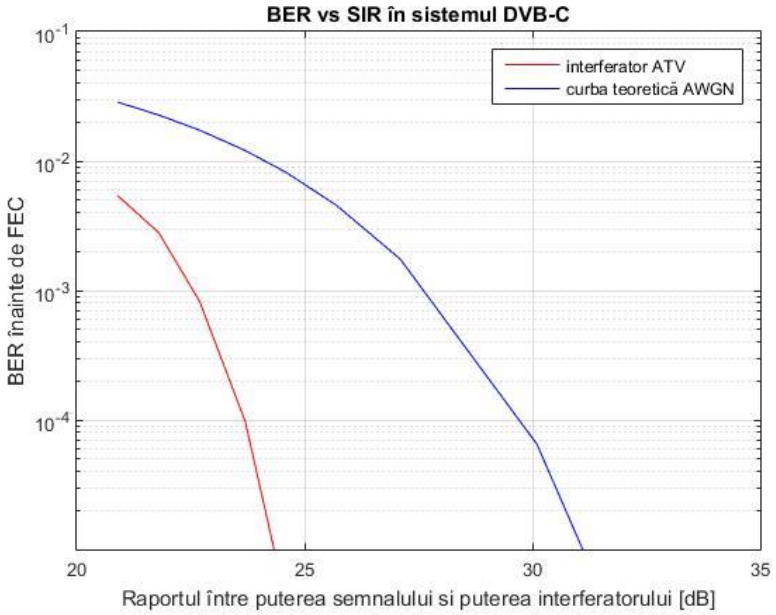

Fig. 19 DVB-C signal interfered with analog TV signal [15]

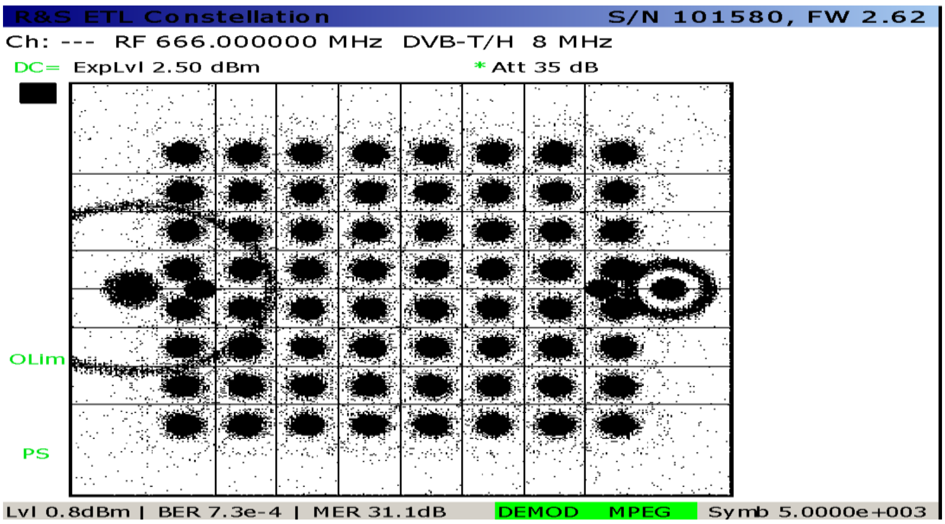

Fig. 20 The effect of unmodulated ATV interferer on 64QAM DVB-T constellation [15]

4. Aplication of Metamaterials in Automotive Industry

Chapter 4 is structured in two parts: the first part describes a shielded box made up of metamaterials and the second part a directional coupler made of metamaterials.

In the first part we proposed a solution for suppressing resonant cavity modes in metal boxes designed to protect high frequency circuits. This solution was based on metamaterial technology and presented the new feature of operation starting with zero frequency (dc). Depending on geometric parameters and materials, the operational bandwidth could be higher than 10 GHz.

We evaluated the properties of the proposed structure both in terms of metamaterials, ie by the actual analysis of an infinite periodic repetition of the unit cell and considering two examples of applying a finite version of the closed structure to a metal box with the circuit must be protected.

The two approaches have proven to be consistent. The proposed solution can be applied to shield the circuits that occupy a place close to the axis of the box in parallel with the direction of the signal flow [16], [17], [18].

In the second part we have exploited the possibility of elaborating periodic structures with EBG, which can be used as screens for the realization of a directional coupler for testing Electromagnetic Compatibility. The originality of the proposed solution lies in the fact that the screens operate at a low frequency starting at zero frequency (dc), unlike the solutions found in the literature, which operate in a band between two different frequencies of zero. In fig. 21 one can observe the directional coupler having 11 unit cells in the direction of the signal flow and 8 cells in the orthogonal direction.

We presented the results obtained on S parameters calculated using CST Microwave Studio [19], which demonstrates the correct operation of the structure. For example, in fig. 22, parameter S11 indicates that the operation of the device is not affected by resonant cavity modes up to a frequency of approximately 4.78 GHz.

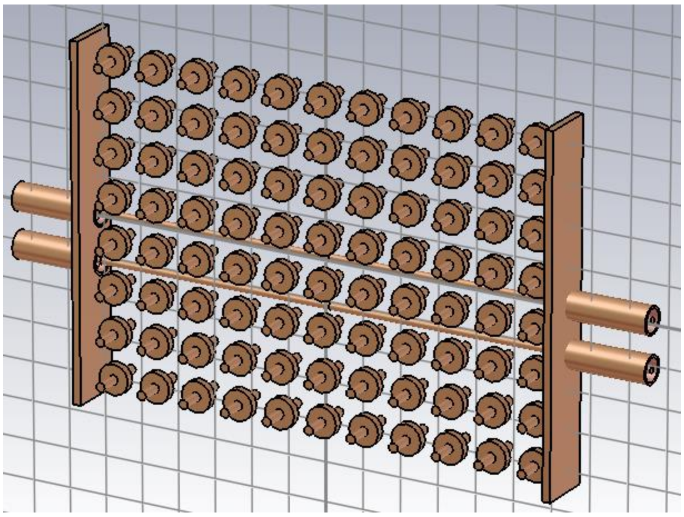

Fig. 21 Directional coupler devised in CST Microwave Studio

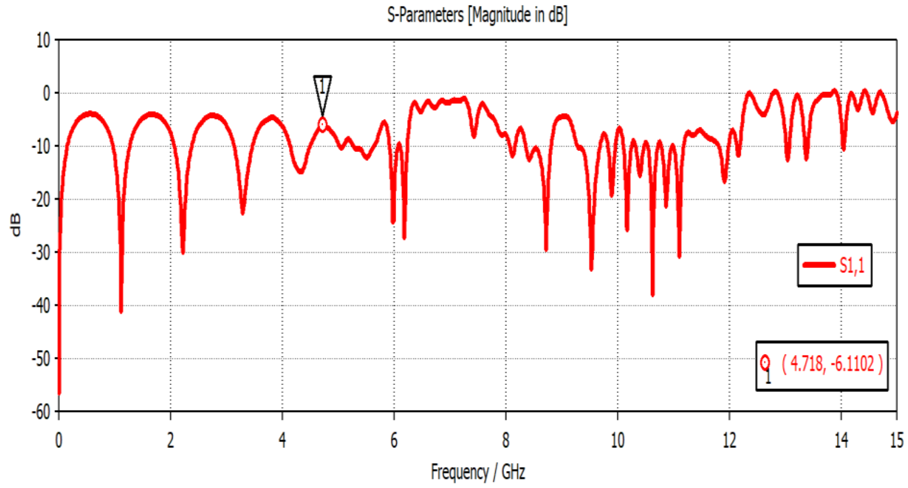

Fig. 22 S11 parameter simulated

We have conducted parametric studies to improve the directional couplers operation. In another particular case (fig. 23) we wanted to see the influence of using a single coaxial line and increasing the number of unit cells. Unlike fig. 21 we used 15 unit cells in the direction of signal flow and 14 cells in the orthogonal direction. The device operates correctly up to 6 GHz. Between 6 and 8 GHz cavity modes are launched.

And this new structure was evaluated according to the metamaterial procedures (calculation of the dispersion diagram) [20]. We have developed the dispersion diagram through the eigenensolver from CST Microwave Studio for the following cases: cell unit, cell unit and a metallic conductor and unit cell and two metallic conductors covering all of the previously described configurations. As shown in the third DD (fig. 24), there are two modes starting from dc: the first mode up to 6 GHz and the second up to 11GHz. These two modes starting from dc correspond to the presence of the two conductors. The second conductor results in the disappearance of the EBG, the effect of its presence on the other modes being quite small.

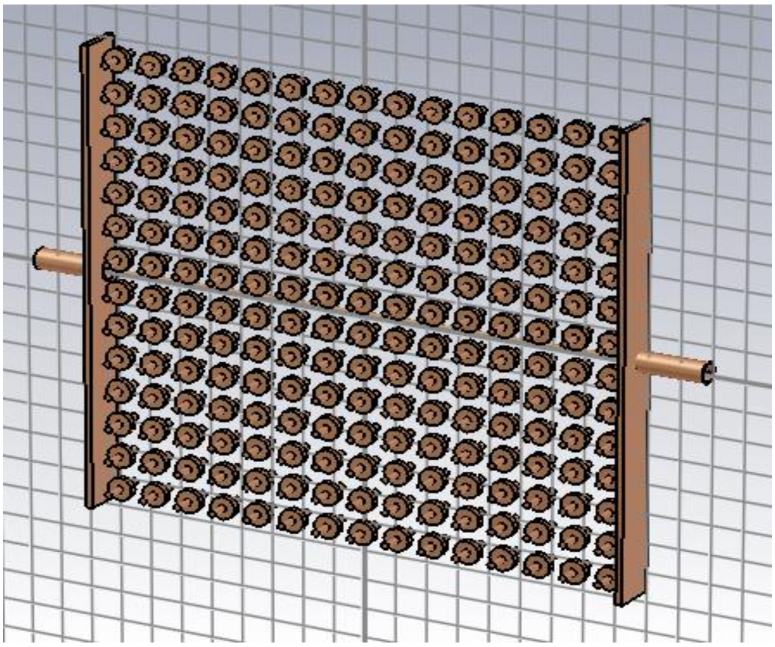
Fig. 23 Modified screening box

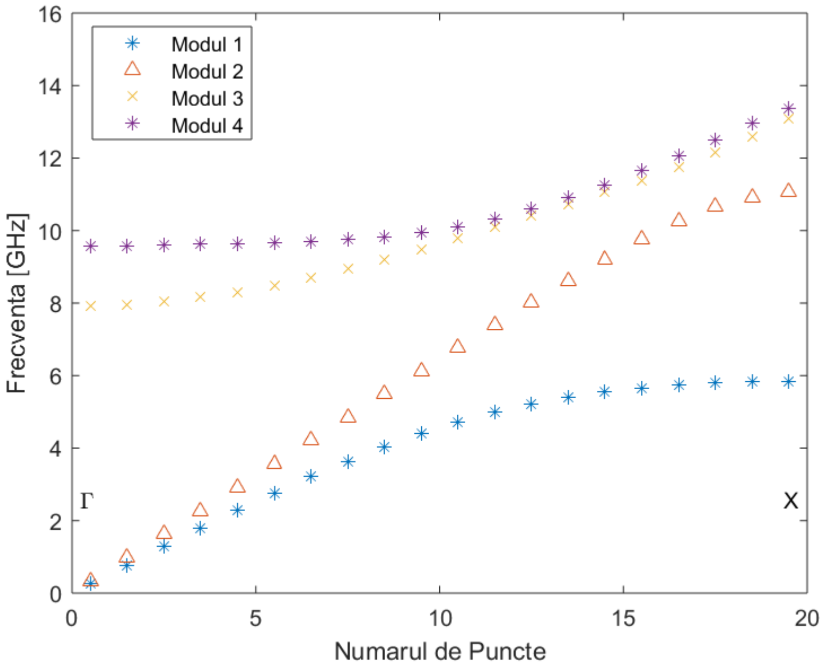

Fig. 24 Dispersion diagram obtained by infinite repetition of the structure

We did not pursue the optimization of the couplers parameters but only demonstrating the feasibility of the concept. The parametric study to provide design data will be the subject of further research. Finally, the directional coupler was practically realized, its S parameters were measured with a network analyzer, and by comparing the practical results with the simulation results we could see good correspondence. The box with two coaxial lines from fig. 21 was made in the Laboratory of the Department of Electronics and Telecommunications of the Polytechnic of Turin, Italy (representation in fig. 25).

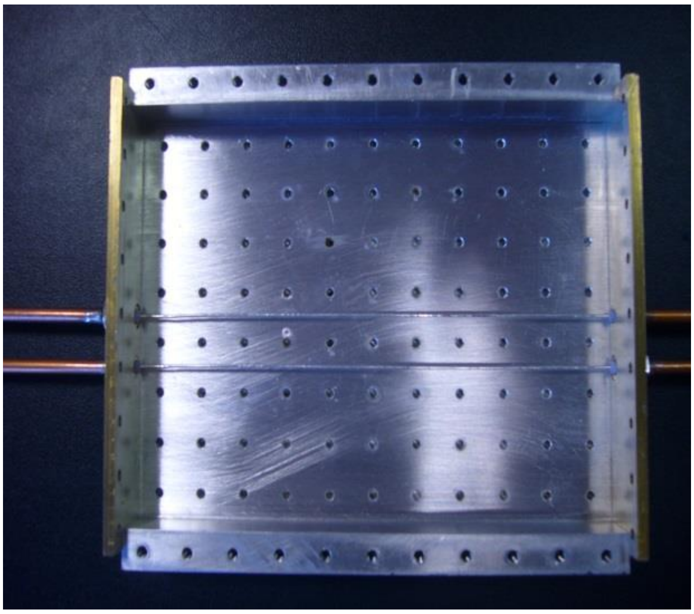

Fig. 25 Inside of the box

We compared the results of S parameters from CST Microwave Studio to those measured in the laboratory using an Agilent Network Analyzer. Fig. 26 shows the comparison of the practical measurements made with the network analyzer and the simulations of the CST Microwave Studio program (parameters S11, S21 and S41). The figure shows a good correlation between simulations and measurements.

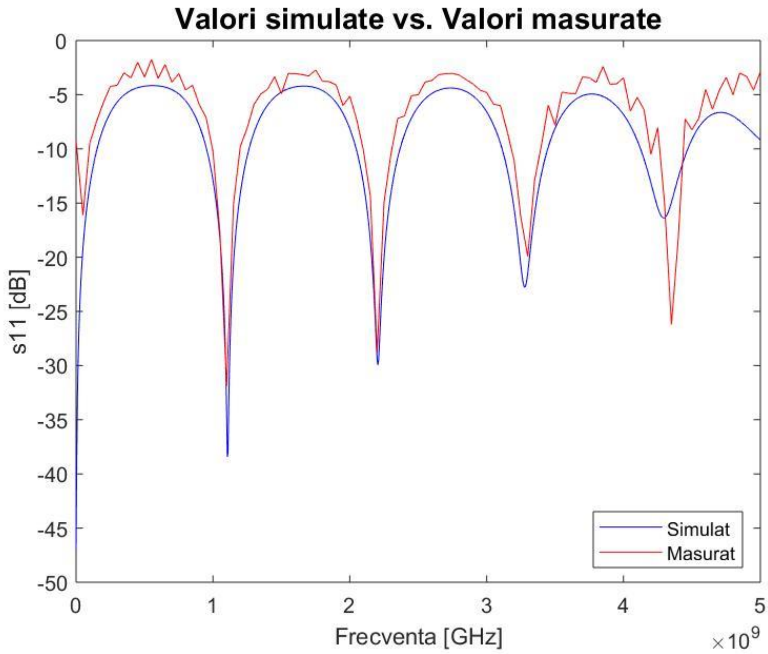

Fig. 26 Simulation and measurement up to 5 GHz. S11 parameter

5. Contributions

During the doctoral program I studied 116 bibliographic titles and also published 2 articles in ISI journals (one of which was accepted for publication in an ISI Q1 - IEEE Access magazine), 15 ISI Proceedings indexed articles, 2 articles in BDI journals and 5 articles at BDI-indexed conferences. I would like to point out that an article in the thesis was quoted in IEEE Transactions on Electromagnetic Compatibility (ISI journal indexed Q3). I enumerate below my own contributions to this thesis.

In the introductory chapter:

- We have presented and commented on relevant aspects of the two standards that are mainly used in the field of Electromagnetic Compatibility of Road Vehicles: CISPR 25 and ISO 11452.
- We presented and commented on the following test methods in the CISPR 25 standard: Emissions Tests (with Absorber Lined Shielded Enclosure and Stripline), Sub-Chapter 1.3, Voltage Testing (Sub-Chapter 1.4) and Emissions with a current probe (sub-chapter 1.5).
- We have also described from ISO 11452 standard, ISO 11452-2 (Absorber Lined Shielded Enclosure), sub-chapter 1.7, ISO 11452-4 (Bulk Current Injection), sub-chapter 1.8 and ISO 11452-5 (Stripline), sub-chapter 1.9.

In chapter 2:

- We have presented and commented on the main Electromagnetic Compatibility Tests regarding radiated and conducted emissions performed in the Automotive Industry and conducted a bibliographic study at the beginning of each sub-chapter.

- Instead of a general theoretical presentation, easy to find in the literature, I chose to describe and comment on the concrete tests I took part, as well as their assessment from different points of view with uncertainty and repeatability.
- We also presented our own contributions to this issue so far:
  - Configuration of the test setup based on measured data with different antennas, measurements made to determine which of the antennas best fit in the given application;
  - presentation of the main equipment used for testing according to the general CISPR 25 radiated emissions standard and the measurement configuration on the basis of previous measurements that have assessed the performance of the equipment (eg antennas);
- Sub-chapters 2.2 and 2.3 describe, study and ameliorate a measurement setup for radiated emissions produced from a car module. It also investigates the differences that occur when different measuring antennas and different semi-anechoic chambers are used in the radiated emission tests performed on the same DUT; for example, a comparison was made between the biconical and log-periodic antenna factors and between the log-periodic and the horn.
- In subchapter 2.4, we presented and commented on some case studies and investigated various methods that can be used to reduce the conductdd emission levels (CE): connect capacitors with values between 10 and 220 nF on the left, left and right screws and the right side of the PCB (the screws to which the PCB metallic case is attached); removing mechanical capacitors and also replacing coils with some shielded ones.
- Also in Chapter 2, in subchapter 2.5, we presented a near-field scanning technique to find solutions for reducing the levels of radiated emissions so as to reduce the time to market of the product; we have presented far field and near field measurement results as well as electromagnetic radiation reduction solutions for the product.
- Finally, a semi-anechoic chamber validation method is presented and discussed in subchapter 2.6, and the results are compared with those obtained in other laboratories.
- The use of chamber debugging techniques in the monopole antenna range was also presented, since initially, too many electromagnetic field peaks were found beyond the accepted limits,.

In chapter 3:

- In subchapter 3.2 we presented and commented on key concepts for testing the immunity of electronic equipment in the Automotive industry to electromagnetic radiation. We started with the definition of immunity and continued with the chain of equipment used for testing in accordance with ISO 11452-2. We chose a radiated immunity test on a Automotive DUT to assess its performance in the presence of an electromagnetic field inside a semi-anechoic chamber.
- We presented the results of the measurements obtained with two different types of antennas in our laboratory: the log-periodic antenna and the horn antenna. Based on these results, we set up realistic calibration methods and test procedures with improved reliability because the equipment parameters were known by measurement and not only by the manufacturer's data.
- In subchapter 3.3 we presented some key concepts for testing the immunity of electronic equipments from modern vehicles to the emissions of portable transmitters. We started with the presentation of the procedure used for testing,

based on ISO-11452-9. After that, we compared two directional couplers to see which one is best suited to this application.

- We also measured the VSWR and presented Smith charts corresponding for three helical antennas commonly used for immunity testing to see if they correspond to the manufacturer's nominal values. Finally, we tested the two directional couplers and the three antennas and concluded that it is advisable to use a Werlatone coupler to achieve more realistic results.
- We have demonstrated the need to rely on the measured parameters of the equipment instead of the nominal values of the manufacturer's specifications in order to avoid potential falsified results of the immunity tests.
- In subchapter 3.4 we tested the effects of CW, FM and analogue (ATV) signals on DVB-T and DVB-C channels when they act as additive noise. We made BER vs. SIR comparisons in all three cases.
- We presented the spectrum of a DVB-T signal interfering with an ATV signal having the same channel power (DVB-T channel power is equal to the channel power of the ATV interferer). We also illustrated the impact of an unmodulated and modulated ATV interfering on the 64QAM DVB-T constellation.

In chapter 4:

- In subchapter 4.2 we presented a solution for suppressing resonant cavity modes in metal boxes designed to protect high-frequency circuits. This solution was based on metamaterial technology and presented the new feature of operation starting with dc. Depending on geometric parameters and materials, the operational bandwidth could be higher than 10 GHz.
- We evaluated the properties of the proposed structure from the perspective of metamaterials, ie by the actual analysis of an infinite periodic repetition of the unit cell and taking into account two examples of applying a finite version of the closed structure to a metal box with the circuit be protected.
- In subchapter 4.3 we have exploited the possibility to develop periodic EBG structures that can be used as screens for making a directional coupler for Electromagnetic Compatibility testing. The originality of the solution lies in the fact that the shields operate at a low frequency starting at zero frequency (dc), unlike the solutions presented in the literature, which operate between two different frequencies of zero.
- In subchapter 4.3.2 we presented the results obtained with S parameters simulated using the CST Microwave Studio, which demonstrates the operation of the structure.
- In subchapter 4.3.3 we presented the results of some parametric studies performed to test and possibly improve the operation of the coupler: elimination of some cell rows, introduction of discontinuities, and use of a single coaxial line with multiple unit cells inside the box.
- And this new structure was evaluated according to the metamaterial procedures (calculation of the dispersion diagram, sub-chapter 4.3.5): cell unit, cell unit and a metal conductor and unit cell and two metallic conductors, to cover all previously presented configurations .
- Finally, in subchapter 4.3.6, we described how the directional coupler was practically realized, its S parameters were measured with a network analyzer, and a good correspondence could be observed by comparing the practical results with the simulation results.

6. References

1. International Standard CISPR 25, “Vehicles, boats and internal combustion engines - Radio disturbance characteristics - Limits and methods of measurement for the protection of on-board receivers”, 3.0 ed. 2008.
2. A. Schwab, W. Kurner, *Electromagnetic Compatibiity,* Bucureşti: AGIR, 2013 (in Romanian translated from German).
3. ISO 11452-1:2005 Road vehicles - Component test methods for electrical disturbances from narrowband radiated electromagnetic energy: International Standardization Organisation, 2005, Part 1: General principles and terminology.
4. ISO 11452-2:2004 Road vehicles - Component test methods for electrical disturbances by narrowband radiated electromagnetic energy: International Standardization Organisation, 2004, Part 2: Absorber-Lined Shielde Enclosure.
5. ISO 11452-4:2011 Road vehicles - Component test methods for electrical disturbances by narrowband radiated electromagnetic energy: International Standardization Organisation, 2011, Part 4: Harness excitation methods.
6. ISO 11452-5:2002 Road vehicles - Component test methods for electrical disturbances by narrowband radiated electromagnetic energy: International Standardization Organisation, 2002, Part 5: Stripline.
7. **A. SILAGHI**, E. Tolan, A. De Sabata, A. Buta, „Measurement of radiated emissions from an automotive cluster”, Electronics and Telecommunications (ISETC), 2016 12th IEEE International Symposium on, 27-28 Oct 2016, Timisoara, Romania, pp. 21-24, 2016.
8. **A. SILAGHI**, C. Balan, E. Tolan, A. De Sabata, „The influence of measurement setups in radiated emissions testing”, Engineering of Modern Electric Systems (EMES), 2017 14th International Conference on, 1-2 June 2017, Oradea, Romania, pp. 220-223, 2017.
9. **A. SILAGHI**, A. Buta, S. Baderca, A. De Sabata, „Methods for reducing Conducted Emissions levels”, 22nd IMEKO TC4 International Symposium and 20th International Workshop on ADC Modelling and Testing 2017, 14-15 September 2017, Iasi, Romania, 2017, pp. 352-355.
10. **A. SILAGHI**, R. Aipu, A. De Sabata, P. M. Nicolae, „Near-field scan technique for reducing Radiated Emissions in Automotive EMC: A Case Study”, 2018 IEEE International Symposium on Electromagnetic Compatibility and 2018 IEEE Asia-Pacific Symposium on Electromagnetic Compatibility (EMC/APEMC 2018), 14-18 May 2018, Singapore, Singapore, 2018, pp. 831-836.
11. **A. SILAGHI**, R. Aipu, A. De Sabata, F. Alexa, „Absorber Lined Shielded Enclosure Chamber Validation”, 2018 13th International Symposium on Electronics and Telecommunications (ISETC 2018), 8-9 November 2018, Timisoara, Romania, 2018.
12. **A. SILAGHI**, A. De Sabata, F. Alexa, A. Buta, S. Baderca, „Measurement of radiated immunity in the automotive industry: Key concepts”, Electronics and Telecommunications (ISETC), 2016 12th IEEE International Symposium on, 27-28 Oct 2016, Timisoara, Romania, pp. 25-28, 2016.
13. **A. SILAGHI**, A. De Sabata, M. Silaghi, „Testing Immunity to Portable Transmitters with Helical Antennas: Key concepts”, 2016 IEEE 22nd International Symposium for Design and Technology in Electronic Packaging (SIITME 2016), 20-23 October 2016, Baile Felix, Oradea, Romania, 2016, pp. 270-273.
14. **A. SILAGHI,** T. Petrita, U. L. Rohde, M. Silaghi, „Performance of the reception of DVB signals in the presence of a communication signal interferer”, 2014

International Symposium on Electromagnetic Compatibility (EMC Europe 2014), 1-4 September 2014, Gothenburg, Sweden, 2014, pp.164-168.
15. **A. SILAGHI**, F. Alexa, T. Petrita, H. Silaghi, M. Silaghi, "DVB demodulation in presence of analogic interferer", 2014 11th International Symposium on Electronics and Telecommunications (ISETC 2014) , 14-15 November 2014, Timisoara, Romania, 2014,pp.1-4.
16. D. Sievenpiper, L. Zhang, F. J. Boas, N. G. Alexópoulos, E. Yablonovitch, "High-impedance electromagnetic surfaces with a forbidden frequency band", IEEE Trans. MTT, vol. 47, no. 11, pp. 2059-2074, Nov. 1999.
17. A. De Sabata, L. Matekovits, **A. SILAGHI**, „Metamaterial based screening box working from DC up to GHz range”, 2015 International Symposium on Signals, Circuits and Systems (ISSCS 2015), 9-10 July 2015, Iasi, Romania, pp. 1-4, 2015.
18. A. De Sabata, L. Matekovits, "Reduced complexity biasing solution for switched parallel-plate waveguide with embedded active metamaterial layer", Journal of Electromagnetic Waves and Applications (JEMWA), vol. 26, no. 14/15, pp. 1828-1836, 2012.
19. www.cst.com
20. L. Brillouin, *Wave Propagation in Periodic Structures*, New York: Dover, 1953.